

**Impurity-induced spin gap asymmetry in nanoscale graphene**

Julia Berashevich and Tapash Chakraborty\*

*Department of Physics and Astronomy, University of Manitoba, Winnipeg, Canada R3T 2N2*

(Received 17 June 2009; revised manuscript received 26 August 2009; published 25 September 2009)

We present a way to control both the band gap and the magnetic properties of nanoscale graphene, which might prove highly beneficial for application in nanoelectronic and spintronic devices. We have shown that chemical doping by nitrogen along a single zigzag edge lowers the symmetry from  $D_{2h}$  (pure graphene) to  $C_{2v}$ , thereby accommodating the state with antiferromagnetic spin ordering of localized states between the zigzag edges. This leads to an increase in the gap in comparison to that of pure graphene in its highest possible symmetry of  $D_{2h}$  and a shift of the molecular orbitals localized on the doped edge in such a way that the spin gap asymmetry, which can lead to half metallicity under certain conditions, is obtained. The doping in the middle of the graphene layer along the zigzag edge results in an impurity level between the highest occupied molecular orbital and lowest unoccupied molecular orbital of pure graphene (much like in semiconductor systems) thus decreasing the band gap and adding unpaired electrons, which can also be used to control the graphene conductivity.

DOI: [10.1103/PhysRevB.80.115430](https://doi.org/10.1103/PhysRevB.80.115430)

PACS number(s): 73.22.-f, 73.20.Hb, 73.21.La, 75.25.+z

**I. INTRODUCTION**

Applications of graphene with its unique physical properties<sup>1-5</sup> in nanoelectronics,<sup>6,7</sup> magnetism, and spintronics,<sup>8-12</sup> hang crucially on its band gap and spin ordering at the zigzag edges. A band gap can be opened in graphene by breaking certain symmetries. For example, interaction of graphene with its substrate, such as SiC, leads to the charge exchange between them which breaks the sublattice symmetry.<sup>13</sup> Moreover, the quantum confinement effect also has been found to introduce a small band gap in graphene nanoribbons,<sup>14</sup> just as was predicted earlier theoretically.<sup>15-18</sup> The effect of band gap opening and spin ordering between the zigzag edges are found to be directly linked to each other.<sup>19</sup> When the spins align along the zigzag edges and spin states localized at opposite edges have the same spin orientation, then the symmetry of graphene is preserved and the system is gapless. Otherwise, if the spin-up states are localized along one zigzag edge while the spin down along the other, the sublattice symmetry is broken which leads to a gap. In the light of a recent breakthrough in fabrication of nanoribbons of required size through unzipping of carbon nanotubes, the nanoribbons and nanoscale graphene are the most promising systems for application in nanoelectronics.<sup>20</sup>

Manipulation of the spin ordering is important for both graphene magnetism and its electronic properties. There are several approaches which have been proposed recently to control the spin ordering along the edges.<sup>21-27</sup> One of them is the termination of the zigzag edges by functional groups.<sup>21</sup> This has the advantage that one can achieve half metallicity in this process. However, there are some serious issues involved here. First, many of these functional groups are placed out of the graphene plane thus making the whole structure nonplanar and, most importantly, termination was applied to every second edge cell, which makes its technological application very difficult. In fact, we found that the strong interactions of the graphene lattice with some of the functional groups, such as  $\text{NH}_2$  and  $\text{NO}_2$ , lead to buckling of

the graphene layer and twisting of the functional groups, which subsequently may result in the disappearance of the half metallicity of graphene. The edges of graphene layer were found curl up in earlier studies as well,<sup>27</sup> where the boundary conditions were found to control the planarity of graphene, namely, the curling occurs for stand-alone systems. For nanoscale graphene the ferromagnetic ordering of the spin states along the zigzag edges can also be achieved by adsorption of gas and water molecules on the graphene surface, as shown in our previous work.<sup>22</sup> The adsorption leads to pushing of the  $\alpha$ - and  $\beta$ -spin states to opposite zigzag edges thereby breaking sublattice symmetry and opening a gap. In some cases the spin asymmetry can also occur. For example, adsorption of HF gas molecules provides a highest occupied molecular orbital (HOMO)-lowest unoccupied molecular orbital (LUMO) gap of 2.1 eV for the  $\alpha$ -spin state and 1.2 eV for the  $\beta$ -spin state. However, due to the weak interactions between the adsorbate and the graphene surfaces, the phenomena of the spin alignment along the edges take place locally, thus limiting its potential for application.

The connection between the phenomena of band-gap opening and spin ordering with the sublattice symmetry leads us to conclude that breaking of this symmetry is the main direction to achieve the required semiconductor-type band gap in graphene and a tunable spin ordering. Here we propose that chemical doping along a single zigzag edge can lower the symmetry from  $D_{2h}$  to  $C_{2v}$  symmetry, the latter being characterized by the broken sublattice symmetry, a semiconductorlike gap and antiferromagnetic spin ordering between the zigzag edges. This method is far superior to earlier approaches involving edge termination by functional groups because doping can be done for every unit cell along the zigzag edge and thereby preserves the planarity of graphene. Doping not only breaks the sublattice symmetry of graphene, it can also induce the spin gap asymmetry due to the energetic shift of the molecular orbitals localized on the doped edge. In a structure with a broken symmetry, the  $\text{HOMO}_\alpha$  and  $\text{LUMO}_\beta$  states are localized at one edge while  $\text{HOMO}_\beta$  and  $\text{LUMO}_\alpha$  are at the other. Suppose the doping shifts the  $\text{HOMO}_\alpha$  and  $\text{LUMO}_\beta$  states localized at one edge

down, then the HOMO $_{\alpha}$ -LUMO $_{\alpha}$  band gap ( $\Delta_{\alpha}$ ) is increased while  $\Delta_{\beta}$ , in contrast, will be reduced. If a certain type of impurities can cause a significant shift of the bands, then the half metallicity of graphene may occur. This is what we set out to investigate here. One of the important advantages of this approach is that we expect insensitivity of spin-selective behavior to the quality of the edges, when the band shift induced by the impurities is stronger than the contribution from the edge defects. We also investigate the possibility of obtaining an impurity level in the middle of the graphene band gap (in analogy to semiconductors) by substitutional doping of a row of carbon atoms along the zigzag edge, which has a lot of technological possibilities as well. Our study of nanoscale graphene was based on the quantum chemistry methods using the spin-polarized density-functional theory with the semilocal gradient corrected functional (UB3LYP/6-31G) performed in the Jaguar 7.5 program.<sup>28</sup>

## II. SYMMETRY OF NANOSCALE GRAPHENE

The highest symmetry for bulk graphite is the hexagonal symmetry while for nanoscale graphene it would be the  $D_{2h}$  planar symmetry with an inversion center. Additionally, there are other lower symmetry classes available for nanoscale graphene, such as the  $C_{2v}$  symmetry with the mirror plane of symmetry perpendicular to the zigzag or armchair edges, only the planar symmetry,  $C_s$  and no symmetry,  $C_1$ . It has been shown in others nanoscale systems<sup>29</sup> that they can be tailor made with a desired symmetry. The lowest-energy structure of graphene is found to be with  $C_s$  or  $C_1$  symmetries, which is of much lower energy (about 2.0 eV for structures with different sizes) than that of the  $C_{2v}$  symmetry state with the mirror plane perpendicular to the zigzag edges. However, controllable spin ordering along the edges occurs only for the high-symmetry states, such as the  $D_{2h}$  planar symmetry and the  $C_{2v}$  symmetry, which are most interesting from the point of view of device applications and will be the subject of our present work. Further, we chose only one state of graphene with  $C_{2v}$  symmetry where the mirror plane is perpendicular to the zigzag edges, which is characterized by a much lower total energy than that with the mirror plane perpendicular to the armchair edges ( $\sim 1.5$  eV). This symmetry type is characterized by the ferromagnetic spin ordering along the zigzag edges and antiferromagnetic spin ordering between the opposite zigzag edges that has potential application of the graphene in spintronics.<sup>8,9,30,31</sup> The graphene structure optimized with constraints associated with  $D_{2h}$  and  $C_{2v}$  symmetries would be characterized by a different lattice. However, for nanoscale graphene optimized with  $D_{2h}$  symmetry the breaking of the sublattice symmetry can cause a spontaneous transfer of graphene to the state of  $C_{2v}$  symmetry. That can be achieved with unequal doping of the graphene sublattices as a result of interaction of the graphene surface with adsorbed molecules<sup>22</sup> or with the substrate.<sup>13</sup> However, it also can be done in controllable way inducing lattice dissimilarity between sublattices, that is, under consideration in present work.

The  $D_{2h}$  symmetry results in structurally identical corners exhibiting ferromagnetic ordering of the spin-polarized states

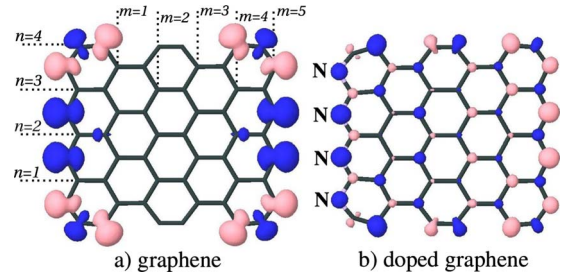


FIG. 1. (Color online) The spin-density distribution: (a) for nanoscale graphene optimized with the  $D_{2h}$  point-group symmetry and (b) for the case when one edge is doped by nitrogen, where the highest symmetry is the  $C_{2v}$  symmetry. Different colors indicate the  $\alpha$ - (light) and  $\beta$ -spin (dark) states. The spin density is plotted for isovalues of  $\pm 0.01$  e/ $\text{\AA}^3$ . The  $n$  and  $m$  are introduced to identify the number of the carbon rings along the zigzag edge ( $n$ ) and along the armchair edge ( $m$ ).

localized at the corners, as shown in Fig. 1(a). According to the NBO (natural bond orbital) analysis, the localized electrons at the corners are unpaired  $sp$  electrons belonging to nonbonded orbitals that are located at the bottom of the conduction band or top of the valence band. For this symmetry, both the  $\alpha$ - and  $\beta$ -spin states of the HOMO and LUMO are localized along the zigzag edges but their spin density is equally distributed between the two edges. For nanoscale graphene with  $D_{2h}$  symmetry the HOMO-LUMO gap appears due to the confinement and the edge effects.<sup>15</sup> The degeneracy of the  $\alpha$ - and  $\beta$ -spin states belonging to the HOMO and LUMO depends on the edge configuration, i.e., the  $\alpha$  and  $\beta$  states can be nondegenerate or degenerate depending on the number of the carbon rings along the zigzag and armchair edges.<sup>22</sup> The degeneracy reappears for larger structures, such as  $n \geq 8$  and  $m \geq 7$  [see notation in Fig. 1(a)]. An increase in the graphene size leads to disappearance of the confinement effect and as a result the gap vanishes. Therefore, for  $n=4$  and  $m=5$  the gap is  $\sim 0.5$  eV and already for  $n=6$  and  $m=7$  the gap is suppressed to  $\sim 0.19$  eV. The influence of the confinement effect on the graphene gap has been already confirmed experimentally.<sup>14</sup>

However, the state with  $D_{2h}$  symmetry is not the energetically preferable state for nanoscale graphene. Graphene, optimized with the  $C_{2v}$  symmetry, where the mirror plane of symmetry is perpendicular to the zigzag edges, has a total energy that is lower than that for the  $D_{2h}$  symmetry. For the  $C_{2v}$  symmetry, the HOMO and LUMO are characterized by the  $\alpha$ - and  $\beta$ -spin states localized on the opposite zigzag edges. Since the carbon atoms at the opposite zigzag edges belong to different sublattices, such spin distribution breaks the sublattice symmetry and a gap opens ( $\sim 1.63$  eV for  $n=4$  and  $m=5$ ). The size of the gap is comparable to that found for nanoribbons,<sup>15</sup> where for a width of  $\sim 10$   $\text{\AA}$  that corresponds to  $n=4$  in our work, the gap was about 1.0 eV. The larger gap of nanoscale graphene obtained here is a result of significant contribution from the confinement effect, as the system is confined in all directions.

The localization of the  $\alpha$ - and  $\beta$ -spin states belonging to HOMO and LUMO at the opposite zigzag edges is important for its possible application in spintronics.<sup>8,9,30,31</sup> However,

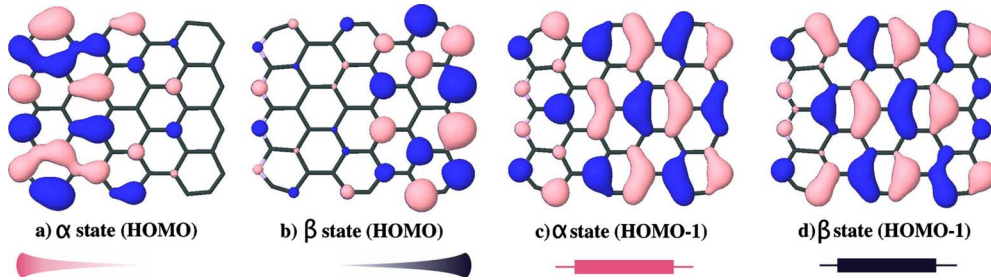


FIG. 2. (Color online) Spin polarizations in nanoscale graphene where the left edge is doped by nitrogen. Different colors correspond to different signs of the molecular-orbital lobes. The electron densities are plotted for isovalues of  $\pm 0.02 \text{ e}/\text{\AA}^3$ : (a)  $\alpha$  state of HOMO ( $E_{\text{HOMO}} = -6.04 \text{ eV}$ ), (b)  $\beta$  state of HOMO ( $E_{\text{HOMO}} = -5.43 \text{ eV}$ ), (c)  $\alpha$  state of (HOMO-1) ( $E_{\text{HOMO-1}} = -6.38 \text{ eV}$ ), and (d)  $\beta$  state of (HOMO-1) ( $E_{\text{HOMO-1}} = -6.43 \text{ eV}$ ). The HOMO and LUMO are found to be localized at the single zigzag edges (edge states), while (HOMO-1) and (LUMO+1)—delocalized over the entire graphene structure (surface states). Bottom pictures show the representation of the localized and surface states.

the energy difference between the states of the  $D_{2h}$  symmetry and the  $C_{2v}$  symmetry is not significant. For small structures such as  $n=4$  and  $m=5$  the difference is  $\sim 0.5 \text{ eV}$  but it decreases exponentially down to  $\sim 0.02 \text{ eV}$  with increasing structure size of up to  $n \geq 6$  and  $m \geq 7$  that are in good agreement with earlier work.<sup>17</sup> The gap disappears for  $n > 8$  and  $m > 8$ . Therefore, the state of pure graphene with the  $C_{2v}$  symmetry, which is of major interest due to the distribution of the localized states with opposite spin orientation between two zigzag edges, becomes unstable with increasing structure size. However, we have found a way to establish graphene in a state of  $C_{2v}$  symmetry. The distortion or dissimilarity induced along a single zigzag edge not only breaks the sublattice symmetry of the graphene but also lowers the symmetry from  $D_{2h}$  to  $C_{2v}$ , thereby accommodating the graphene in a state characterized by antiferromagnetic spin ordering between the zigzag edges. The spin-density distribution for nanoscale graphene with one zigzag edge doped by nitrogen is presented in Fig. 1(b). Localized states along the zigzag edges are formed by unpaired electrons belonging to the natural nonbonded orbitals, which participate in formation of the HOMO and LUMO. The  $\alpha$ - and  $\beta$ -spin states of the HOMO and LUMO are spatially separated, i.e., localized at opposite zigzag edges. The (HOMO-1) and (LUMO+1) orbitals usually correspond to the surface states, redistributed over the entire graphene structure. The surface states are important for conductivity of graphene in a transverse electric field because the charge transfer between the spatially separated HOMO and LUMO may occur through participation of the surface states. The electron-density distribution for the edge states and the surface states is presented in Fig. 2. The slight difference between the  $\alpha$ - and  $\beta$ -spin surface states (HOMO-1) is due to doping of the left zigzag edge. The  $\alpha$ - and  $\beta$ -spin states remain spatially separated with increasing structure size.

### III. HALF METALLICITY OF GRAPHENE

The edge dissimilarity allows us to explore the required properties, such as the semiconductor-type band gap and localization of  $\alpha$ - and  $\beta$ -spin states at opposite zigzag edges. Moreover, the spatial separation of the  $\alpha$ - and the  $\beta$ -spin

states resulted from doping of the single zigzag edge is stable in comparison to the water adsorption.<sup>22</sup> Doping of a single edge shifts the band energies of the orbitals which are strongly localized at this edge. Such a shift provides an opportunity to obtain another useful property of graphene which is important for spintronics—the half metallicity. For the HOMO or LUMO, which are shown to be localized at the edges, the substitutional doping at the single zigzag edge can create a strong nondegeneracy of the  $\alpha$ - and  $\beta$ -spin states because these states are spatially separated and localized at the opposite edges. Moreover, the  $\text{HOMO}_\alpha$  and  $\text{LUMO}_\beta$  are localized at one edge while  $\text{HOMO}_\beta$  and  $\text{LUMO}_\alpha$  at the other. If doping increases the band gap  $\Delta_\alpha$  for the  $\alpha$ -spin state, then the band gap  $\Delta_\beta$  for the  $\beta$ -spin state, in contrast will be reduced, and vice versa. Therefore, doping induces the spin gap asymmetry in graphene. Materials exhibiting asymmetric gaps for the  $\alpha$ - and  $\beta$ -spin states where one gap is of semiconductor type while the other is an insulator, are known as half-semiconductor materials, but if one of them is metallic, the system is half metallic. Therefore, by choosing the right doping we can achieve a stable half metallicity in graphene which will be an important step forward for applications in spintronics.

We have investigated the transformation of the electronic structure of nanoscale graphene due to the induced edge dissimilarities. The results are schematically presented in Fig. 3. For nanoscale graphene with  $D_{2h}$  symmetry a small band gap occurs due to the confinement. The HOMO and LUMO in this case are localized at the zigzag edges but their electron density is equally redistributed over both edges [see Fig. 3(a)]. Termination of the left zigzag edge by hydrogen [Fig. 3(b)] opens a gap as a result of breaking of the sublattice symmetry, thereby lowering  $D_{2h}$  symmetry to a state of  $C_{2v}$  symmetry. The hydrogenation leads to saturation of the dangling  $\sigma$  bonds at the terminated edge but does not significantly change the energy of the  $\text{HOMO}_\alpha$  and  $\text{LUMO}_\beta$  states localized at this edge. The resulting nondegeneracy of the  $\alpha$ - and  $\beta$ -spin states is not large, and the HOMO-LUMO gap of the  $\alpha$ -spin state ( $\Delta_\alpha = 1.8 \text{ eV}$ ) is almost identical to that of the  $\beta$ -spin state ( $\Delta_\beta = 2.1 \text{ eV}$ ). For pure graphene in a state with  $C_{2v}$  symmetry, the energy diagram differs mostly by the magnitudes of the energy gap  $\Delta_\alpha$  and  $\Delta_\beta$ , which are  $\sim 1.5 \text{ eV}$  for this case. Therefore, hydrogen termination

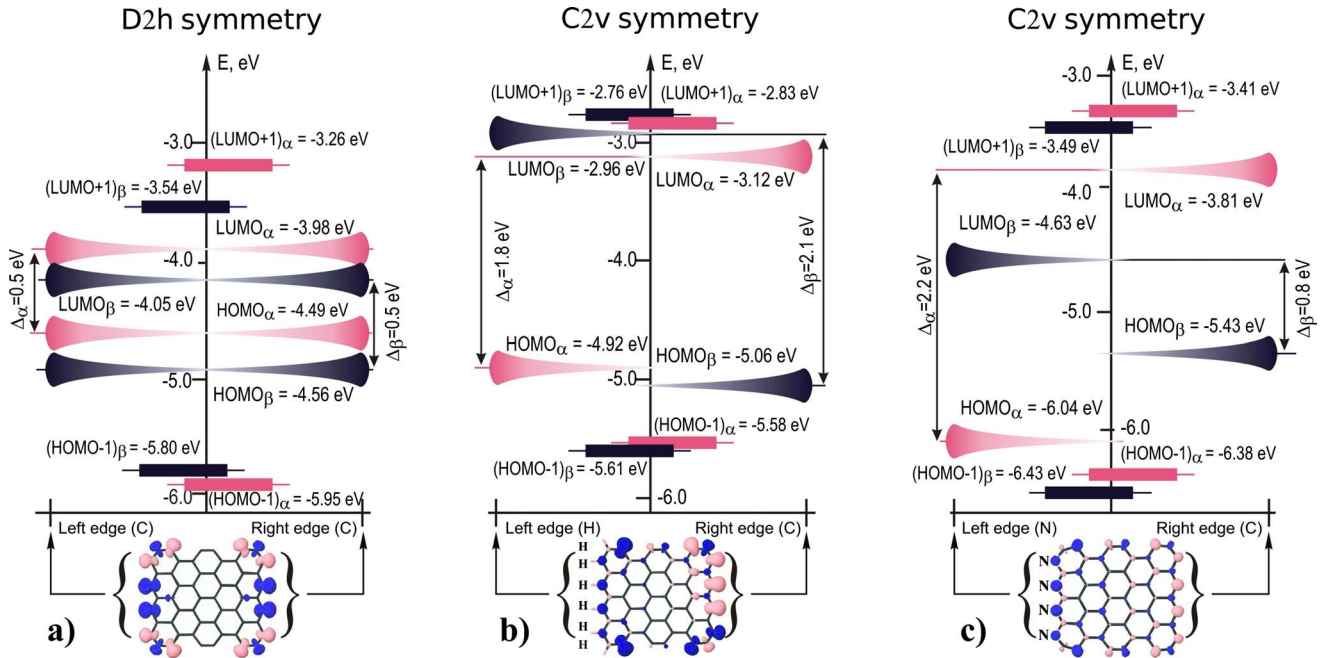


FIG. 3. (Color online) Schematic diagrams showing the distribution of the edge states and surface states in the energy scale and over the graphene structure (see the bottom pictures in Fig. 2 for pictorial description of the states). The structures at the bottom demonstrate the spin distribution with isovalues of  $\pm 0.01 e/\text{\AA}^3$ . (a) Nanoscale graphene optimized with the  $D_{2h}$  symmetry, (b) with left edge terminated by hydrogen, and (c) with the left zigzag edge doped by nitrogen. For the localized states the energy levels (HOMO and LUMO) show density distribution (schematic), particularly delocalization of the orbitals between the two edges if the  $D_{2h}$  symmetry is preserved, and their localization on the zigzag edges when sublattice symmetry is broken and  $C_{2v}$  symmetry becomes to be highest possible symmetry. The surface states [(HOMO-1) and (LUMO+1)] are delocalized over the entire graphene structure [see, for example, Figs. 2(c) and 2(d)].

along a single zigzag edge increases the gap from  $\sim 1.5$  eV for pure graphene in state of  $C_{2v}$  symmetry to  $\sim 1.9$  eV due to major breaking of the sublattice symmetry in comparison to that of pure graphene, where symmetry breaking is induced by the spin distribution.

Doping of the left zigzag edge by nitrogen [see Fig. 3(c)] shifts down the orbital energies of the  $\text{HOMO}_\alpha$  and  $\text{LUMO}_\beta$  states localized at the doped edge and results in a strong nondegeneracy of the orbitals. This leads to a slight enhancement of the HOMO-LUMO gap for the  $\alpha$ -spin state up to  $\Delta_\alpha = 2.2$  eV but a significant decrease in the HOMO-LUMO gap for the  $\beta$ -spin state down to  $\Delta_\beta = 0.8$  eV. The length of the nitrogen-carbon bond at the edges is found to be  $d_{\text{N-C}} = 1.35$  \AA, which is similar to the carbon-carbon bonds  $d_{\text{C-C}} = 1.39$  \AA. Similar results are obtained for the phosphorus impurities, where the gaps are  $\Delta_\alpha = 2.0$  eV and  $\Delta_\beta = 0.9$  eV. Phosphorus is, however, less useful because of the large phosphorus-carbon bond ( $d_{\text{P-C}} = 1.78$  \AA) which can lead to destruction of the lattice. We have also investigated the possibility to dope the single zigzag edge of the nanoscale graphene by other impurities, such as oxygen and boron, but they are not as effective as nitrogen. The oxygen doping leads to strong delocalization of the electron density of the orbitals localized at the edges. The doping by boron leads to destruction of the graphene lattice due to the long boron-carbon bonds at the edges ( $d_{\text{B-C}} = 1.42$  \AA), thereby significantly stretching the doped edge that can lead to breaking of the bonds at the corner of the edges. Doping by boron shifts the states localized at the edges from the HOMO-LUMO gap deeper into the conduction and valence bands.

For the size of the nanoscale graphene investigated in this work, the spin asymmetry is achieved but the band-gap magnitude for  $\alpha$ - and  $\beta$ -spin states corresponds to the half-semiconductor behavior ( $\Delta_\alpha = 2.2$  eV,  $\Delta_\beta = 0.8$  eV). We found that the spin-selective behavior of graphene is preserved with increasing structure size because substitutional doping energetically shifts the orbitals localized on the doped edge independently of the graphene size and breaks the symmetry of graphene. However, increasing the size of graphene results in a decrease in both the  $\Delta_\alpha$  and  $\Delta_\beta$  gaps due to diminishing confinement effects. Therefore, for graphene structures doped by nitrogen or phosphorus of size  $n \geq 6$  and  $m \geq 7$ , the gap  $\Delta_\beta$  is close to being metallic. For  $n = 6$  and  $m = 7$  the gap for  $\alpha$ -spin state is suppressed down to 1.13 eV while for  $\beta$ -spin state down to 0.19 eV, which corresponds to the *half-metallic behavior of graphene*.

An external electric field applied between the zigzag edges has been shown<sup>8,9,30,31</sup> to shift the band of graphene with spatially separated and degenerate  $\alpha$ - and  $\beta$ -spin states. The electric field shifts the bands in such a way that for  $\alpha$  spin the HOMO and LUMO levels move closer to each other in the energy scale while for  $\beta$  spin they move apart. At a certain electric field,  $\Delta_\alpha$  vanishes and the metallic behavior of graphene appears. If the electric field  $+E_c$  can close the band gap for the  $\alpha$ -spin state,  $-E_c$  leads to disappearance of the band gap for the  $\beta$ -spin state. Therefore, the current-voltage characteristic of such a structure will be symmetrical because the  $\Delta_\alpha$  equals  $\Delta_\beta$  and for both spin states the switch from the semiconductor to metallic behavior occurs at the same critical electric field  $\pm E_c$ . The advantage of graphene

with spin gap asymmetry, i.e., different  $\Delta_\alpha$  and  $\Delta_\beta$  gaps, found in this work is that, the different values of the critical electric field required to close these gaps, such that  $|E_{c(\beta)}| < |E_{c(\alpha)}|$  when  $\Delta_\beta < \Delta_\alpha$ . Therefore, this structure will be characterized by the spin-selective behavior and asymmetric spin channels.

#### IV. DOPING OF GRAPHENE

We have also investigated the influence of impurities on the electronic structure of graphene in the case when they are not embedded at the zigzag edges. Replacing the row of carbon atoms by nitrogen atoms in a graphene lattice along the single zigzag edge results in the appearance of impurity levels *inside* of both the  $\Delta_\alpha$  and  $\Delta_\beta$  gaps. The energy diagram of localization of the molecular orbitals for the doped graphene is presented in Fig. 4. As we mentioned earlier, in pure graphene the HOMO and LUMO are localized at the zigzag edges. The applied doping creates one extra occupied orbital (HOMO) which is localized at the embedded nitrogen atoms and located above the occupied orbital belonging to the edges, which becomes HOMO-1. The NBO analysis has shown that this extra orbital is formed by the unpaired *sp* electron localized on each nitrogen atoms. This reduces the HOMO-LUMO gap ( $\Delta_\alpha=1.1$  eV and  $\Delta_\beta=0.7$  eV) while preserving the spin asymmetry.

In an applied in-plane electric field the charge transfer occurs between the orbitals localized on the opposite zigzag edges, i.e., in our case such transfer occurs between the HOMO-1 and LUMO, which is a multistep process with participation of HOMO. Since the gap is decreased and each nitrogen atom adds an unpaired electron into the system due to the doping, the conductivity of graphene would be significantly enhanced and can be controlled as in semiconductor devices.

#### V. CONCLUSION

We have investigated the possibility to control the electronic and magnetic properties of nanoscale graphene. We found that the dissimilarity of the edges induced by doping lowers the symmetry of graphene from  $D_{2h}$  to  $C_{2v}$ , which is characterized by the spin ordering along the zigzag edges and their antiparallel alignment between opposite zigzag edges. Moreover, impurities embedded at a single zigzag edge shifts in the energy scale the molecular orbitals localized at this edge, thereby decreasing the band gap for one spin channel and increasing the other. Under these conditions, the half-metallic behavior can be achieved. Nitrogen

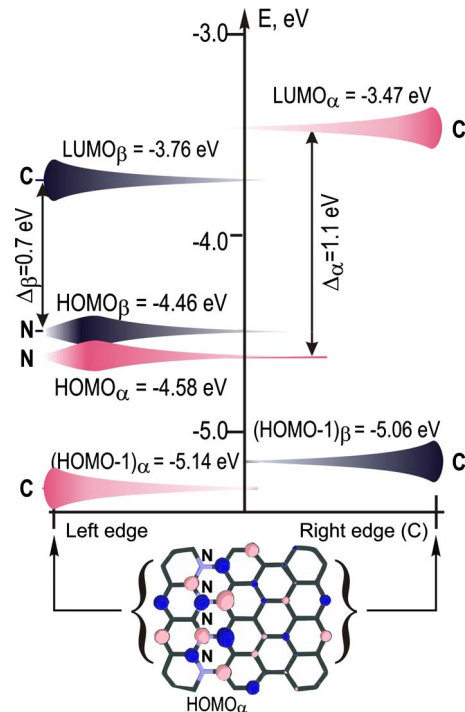


FIG. 4. (Color online) Schematic diagram showing the distribution of the edge states localized on carbon atoms at the graphene edge denoted as “C” in the diagram (LUMO and HOMO-1) and states localized by the dopant in the middle of the graphene structure (HOMO) and denoted as “N” in the diagram (see the bottom pictures in Fig. 2 for pictorial description of the states). The  $HOMO_\alpha$  and  $HOMO_\beta$  are extra impurity levels that appear due to the doping and replaces the occupied orbital localized on the left carbon edge by shifting it deeper into the valence band. The inset picture (in brackets) demonstrates the electron-density distribution for the  $HOMO_\alpha$  with isovalues of  $\pm 0.01$   $e/\text{\AA}^3$ .

doping in the middle of the graphene surface is found to have the prospect for application in nanoelectronics due to the appearance of the occupied impurity levels in the band gap. The impurity level results in a decrease in the band gap of  $\sim 2.0$  eV by one half and contains unpaired electrons, which should lead to an enhancement of the conductivity. Therefore, both the conductivity of the nanoscale graphene and its magnetic properties can be controlled by the impurities.

#### ACKNOWLEDGMENTS

The work was supported by the Canada Research Chairs Program and the NSERC Discovery Grant.

\*chakrabort@cc.umanitoba.ca

<sup>1</sup>A. K. Geim and K. S. Novoselov, *Nature Mater.* **6**, 183 (2007).

<sup>2</sup>Y. Zhang, Y.-W. Tan, H. L. Störmer, and P. Kim, *Nature (London)* **438**, 201 (2005).

<sup>3</sup>V. M. Apalkov and T. Chakraborty, *Phys. Rev. Lett.* **97**, 126801 (2006).

<sup>4</sup>X.-F. Wang and T. Chakraborty, *Phys. Rev. B* **75**, 041404(R) (2007).

<sup>5</sup>D. S. L. Abergel and T. Chakraborty, *Phys. Rev. Lett.* **102**, 056807 (2009).

<sup>6</sup>Z. Chen, Y.-M. Lin, M. J. Rooks, and P. Avouris, *Physica E (Amsterdam)* **40**, 228 (2007).

- <sup>7</sup>E. J. H. Lee, K. Balasubramanian, R. T. Weitz, and M. Burghard, *Nat. Nanotechnol.* **3**, 486 (2008).
- <sup>8</sup>Y.-W. Son, M. L. Cohen, and S. G. Louie, *Nature (London)* **444**, 347 (2006).
- <sup>9</sup>E. Rudberg, P. Salek, and Y. Luo, *Nano Lett.* **7**, 2211 (2007).
- <sup>10</sup>P. Esquinazi, D. Spemann, R. Høhne, A. Setzer, K.-H. Han, and T. Butz, *Phys. Rev. Lett.* **91**, 227201 (2003).
- <sup>11</sup>S. Cho, Y. Chen, and M. S. Fuhrer, *Appl. Phys. Lett.* **91**, 123105 (2007).
- <sup>12</sup>V. M. Karpan, G. Giovannetti, P. A. Khomyakov, M. Talanana, A. A. Starikov, M. Zwierzycki, J. van den Brink, G. Brocks, and P. J. Kelly, *Phys. Rev. Lett.* **99**, 176602 (2007).
- <sup>13</sup>S. Y. Zhou, D. A. Siegel, A. V. Fedorov, and A. Lanzara, *Phys. Rev. Lett.* **101**, 086402 (2008).
- <sup>14</sup>M. Y. Han, B. Özyilmaz, Y. Zhang, and P. Kim, *Phys. Rev. Lett.* **98**, 206805 (2007).
- <sup>15</sup>Y.-W. Son, M. L. Cohen, and S. G. Louie, *Phys. Rev. Lett.* **97**, 216803 (2006).
- <sup>16</sup>K. Nakada, M. Fujita, G. Dresselhaus, and M. S. Dresselhaus, *Phys. Rev. B* **54**, 17954 (1996).
- <sup>17</sup>H. Lee, Y.-W. Son, N. Park, S. Han, and J. Yu, *Phys. Rev. B* **72**, 174431 (2005).
- <sup>18</sup>L. Pisani, B. Montanari, and N. M. Harrison, *New J. Phys.* **10**, 033002 (2008).
- <sup>19</sup>L. Pisani, J. A. Chan, B. Montanari, and N. M. Harrison, *Phys. Rev. B* **75**, 064418 (2007).
- <sup>20</sup>D. V. Kosynkin, A. Higginbotham, A. Sinitskii, J. R. Lomeda, A. Dimiev, B. K. Price, and J. Tour, *Nature (London)* **458**, 872 (2009); L. Jiao, L. Zhang, X. Wang, G. Diankov, and H. Dai, *ibid.* **458**, 877 (2009).
- <sup>21</sup>F. Cervantes-Sodi, G. Csányi, S. Piscanec, and A. C. Ferrari, *Phys. Rev. B* **77**, 165427 (2008).
- <sup>22</sup>J. Berashevich and T. Chakraborty, *Phys. Rev. B* **80**, 033404 (2009).
- <sup>23</sup>D. Gunlycke, J. Li, J. W. Mintmire, and C. T. White, *Appl. Phys. Lett.* **91**, 112108 (2007).
- <sup>24</sup>D. W. Boukhvalov and M. I. Katsnelson, *Nano Lett.* **8**, 4373 (2008).
- <sup>25</sup>Er-jun Kan, Z. Li, J. Yang, and J. G. Hou, *J. Am. Chem. Soc.* **130**, 4224 (2008).
- <sup>26</sup>O. Hod, V. Barone, J. E. Peralta, and G. E. Scuseria, *Nano Lett.* **7**, 2295 (2007).
- <sup>27</sup>E.-J. Kan, X. Wu, Z. Li, X. C. Zeng, J. Yang, and J. G. Hou, *J. Chem. Phys.* **129**, 084712 (2008).
- <sup>28</sup>Jaguar, version 7.5. Schrödinger 2007, LLC: New York, NY.
- <sup>29</sup>*Nanoengineering of Structural, Functional and Smart Materials*, edited by M. J. Schulz, A. D. Kelkar, and M. J. Sundarezan (Taylor & Francis, New York, 2005).
- <sup>30</sup>O. Hod, V. Barone, and G. E. Scuseria, *Phys. Rev. B* **77**, 035411 (2008).
- <sup>31</sup>S. Dutta and S. K. Pati, *J. Phys. Chem. B* **112**, 1333 (2008).